1. BACKGROUND

Current practices in assessing structural ability to withhold a nearby surface explosion only considers airblast load. Actually a surface detonation generates both ground shock and ariblast load. Although ground shock usually reaches a structure earlier than airblast load, ground shock and airblast pressure might act on structures simultaneously, especially when the explosion is close to the structure. Therefore, an accurate analysis of structural response and damage to a nearby surface explosion should consider both ground shock and airblast load. However, current design codes and regulations in designing structures against explosions require consideration of only airblast pressure, whereas the ground shock effect on structural responses is neglected. The significance of neglecting the ground shock in the structural response and damage analysis to surface explosion is not well known.

Much attention has been received in study of dynamic response of structures to airblast forces in the last decades. Most of previous studies in analysis of structures against explosions are mainly dependent on empirical formulae or simplified numerical analysis by modeling a structure or a structure member as a SDOF (Single degree of freedom) system (Henrych 1979; TM-5 1986). Only very few studies can be found in the literature that considered simultaneous airblast load and ground shock on structures (e.g., Dowding et al. 1982). In that study, a single degree of freedom system is assumed to substitute a structure system and only linear elastic structural responses were considered (Dowding et al. 1982). Recently, the effects of simultaneous ground shock and airblast forces on structural responses were investigated by using a pseudo tensor material model for reinforced concrete and a nonlinear orthotropic material model for masonry wall (Wu and Hao 2004). However, collapse of structures to blast loads could not be simulated with this model due to the limitation of the material models, although material nonlinearity was also included.

In this paper, the influences of simultaneous ground shock and airblast forces on structural responses are investigated by using a previously developed 3-dimension homogenized material model for a masonry wall, and another material damage model developed for reinforced concrete structures. These material models are programmed and linked to an available computer program LS-DYNA3D through its user subroutine capability. A one-storey masonry infilled RC frame is used as an example in the study. Dynamic response and damage of the example structure to simultaneous ground shock and airblast forces, or separately to ground shock only or airblast forces only are simulated. Response velocity of the structure as well as structural damage are presented and discussed with respect to different scaled distances. The importance of including the simultaneous ground shock and airblast forces in the structural response and damage analysis is discussed.

2. PREDICTION OF GROUND SHOCK AND AIRBLAST PRESSURE

Simultaneous ground shock and airblast forces from a surface explosion on a structure can be estimated by following empirical formulae. For ground shock, a Tajimi-Kanai function representing the power spectrum of its acceleration time histories is expresses as (Wu and Hao 2005a)

$$S(f) = \frac{1 + 4\varsigma_g^2 \frac{f^2}{PF^2}}{(1 - \frac{f^2}{PF^2})^2 + 4\varsigma_g^2 \frac{f^2}{PF^2}} S_o \tag{1}$$

where ζ_g is a parameter governing the power spectral shape; S_o is the amplitude of power spectrum of a white noise; PF is the principal frequency which can be estimated by

$$PF = 465.62(R/Q^{1/3})^{-0.13}\,Hz \quad 0.3 \le R/Q^{1/3} \le 10 \tag{2}$$

where R is the distance in meters measured from the charge center and Q is the TNT equivalent charge weight in kilograms. For airblast loads, the peak reflected airblast pressure on front wall of the structure can be estimated by

$$p_r(h) = p_{ro}(1 - 0.0006 p_{ro}^{0.46} h^2) \qquad p_{ro} \le 10MPa \tag{3}$$

where h is the height of the wall in meters; and p_{ro} is the peak reflected pressure at the bottom of the wall, which is estimated by

$$p_{ro} = 2.85(p_{so})^{1.206} \qquad p_{so} \le 50MPa \qquad (MPa) \tag{4}$$

where p_{so} is the peak pressure in free air from a surface explosion and can be estimated by

$$p_{so} = 1.059\left(\frac{R}{Q^{1/3}}\right)^{-2.56} - 0.051 \qquad 0.1 \le R/Q^{1/3} \le 1 \qquad (MPa) \tag{5}$$

$$p_{so} = 1.008\left(\frac{R}{Q^{1/3}}\right)^{-2.01} \qquad 10 \ge R/Q^{1/3} > 1 \qquad (MPa) \tag{6}$$

For peak airblast pressure on roof, side and rear walls of the structure, they are equal to the peak free air pressure at any point reduced by a negative drag pressure

$$p_{roof} = p_s - Cq_s \tag{7}$$

where q_s is dynamic pressure in the free air and C is the drag coefficient for the roof, and side and rear walls (TM-5 1986). The time lag between the ground shock and airblast pressure reaching the structure is estimated by

$$T_{lag} = 0.34R^{1.4}Q^{-0.2}/c_a - 0.91R^{1.02}Q^{-0.02}/c_p \text{ (s)} \tag{8}$$

where c_a is the sound speed in the air, which is 340 m/s; c_p is the P wave velocity of the rock mass.

3. MATERIAL MODELS FOR RC AND MASONRY

A 3-dimension homogenized material model developed previously is used to model the performance of masonry (Wu and Hao 2005b). It includes the equivalent elastic properties, strength envelope and damage threshold of masonry. The strength envelope of the masonry model includes linear parts

$$\overline{F}_i = \alpha_i I_1 + \sqrt{J_2} - k_i = 0 \qquad i = 1,2,3 \tag{9}$$

and the cap part

$$\overline{F}_4 = (I_1 - p_2)^2 + R^2 J_2 - (p_3 - p_2)^2 = 0 \tag{10}$$

where I_1 is the first invariant of the stress tensor; $\sqrt{J_2}$ is the second invariant of the stress deviator; α_i, k_i, p_1, p_2 and p_3 are material constants; and R is the ratio of major to the minor axis of cap. Table 1 lists these material constant values derived from the previous study. Damage scalar for masonry is defined as

$$D_m = 1 - \exp(-\overline{\beta}(\overline{\varepsilon}^+ - \overline{\varepsilon}_0^+)/\overline{\varepsilon}_0^+) \tag{11}$$

where $\bar{\varepsilon}^{+}$ is the equivalent tensile strain of masonry; $\bar{\beta}$ is a damage parameter, it is set to 0.5; and $\bar{\varepsilon}_0^{+}$ is the threshold strain and it is equal to 2.76×10^{-4}.

Table 1 Material constants of masonry wall

α_1	k_1 (MPa)	α_2	k_2 (MPa)	α_3	k_3 (MPa)	p_1 (MPa)	p_2 (MPa)	p_3 (MPa)	R
-0.78	0.89	-0.54	0.89	-0.17	8.1	-17.1	-66.3	-109.2	2.91

For concrete material, its degradation damage scalar is defined as

$$D = \alpha_t D_t + \alpha_c D_c\,,\ \dot{D}_t > 0\,,\ \dot{D}_c > 0 \ \text{and}\ \alpha_t + \alpha_c = 1 \tag{12}$$

where D_t and D_c correspond respectively to damage measured in uniaxial tension and uniaxial compression states of concrete, and are defined as (Lubliner et al. 1989)

$$D_c = \frac{1}{G_f^c}\int_0^{\varepsilon_c^p} \sigma_c d\varepsilon_c^p \qquad D_t = \frac{1}{G_f^t}\int_0^{\varepsilon_t^p} \sigma_t d\varepsilon_t^p \tag{13}$$

where G_f^c and G_f^t are the total fracture energy per volume in compression and tension and are defined as

$$G_f^c = \int_0^{\infty} \sigma_c\, d\varepsilon_c^p \qquad G_f^t = \int_0^{\infty} \sigma_t\, d\varepsilon_t^p \tag{14}$$

in which σ_c, σ_t are stress-strain curve functions in uniaxial compression and tension for concrete respectively, which can be described with exponential forms; ε_c^p, ε_t^p are the scalar plastic strains in compression and tension; α_c and α_t are the weights. Strain rate effect for concrete can be described by (Lu and Xu 2004)

$$\frac{\sigma_d}{\sigma_s} = 1 + 1.505\,\dot{\varepsilon}^{0.295} \tag{15}$$

in which σ_d is the dynamic uniaxial compressive /tensile strength (MPa), $\dot{\varepsilon}$ is the dynamic strain rate, σ_s is the uniaxial compressive/tensile strength at the quasi-static loading rate.

A bilinear yield model is used for steel, with Young's modulus $E_s = E_{s1}$ in elastic stage and $E_s = E_{s2}$ if the axial stress exceeds the yield stress.

4. NUMERICAL RESULTS

The above numerical models for masonry and reinforced concrete are programmed and linked to LSDYNA as its user defined subroutines in the present study to simulate structural response and damage. A one-storey masonry infilled RC frame is employed in the analysis as an example structure. Fig. 1 shows configuration of the one-storey masonry infilled RC frame. The span length and height of the structure are 5.0 m and 3.3 m, respectively. The roof slab thickness is 150 mm and floor width is 5m. The columns and beams have a cross section of 300*300 mm and 200*300 mm with a 2% reinforcement ratio. The grade of concrete is C30 with the elastic modulus $E_c = 27$ GPa and shear modulus $G_c = 14$ GPa and the reinforcement is Grade S460 with Young's modulus $E_{s1} = 210$ GPa and plastic hardening modulus $E_{s2} = 21$ GPa. The thickness of the masonry wall is 240 mm. The masonry walls are tied to the beam and columns on all sides using a tied failure contact slideline in the simulation. These slidelines keep element faces together until a prescribed failure criterion is reached. The failure criterion was set to be equivalent to known data on the strength of mortar. Targets 1 to 6 on the structure are specified to record dynamic response. The imposed and dead loads of 3 kN/m^2 on structural floors as specified in BS8110 (1985) are also included in the analysis. The charge weight of 1000 kg TNT is used and the structural response to blast loads at different scaled distances is simulated in the analysis.

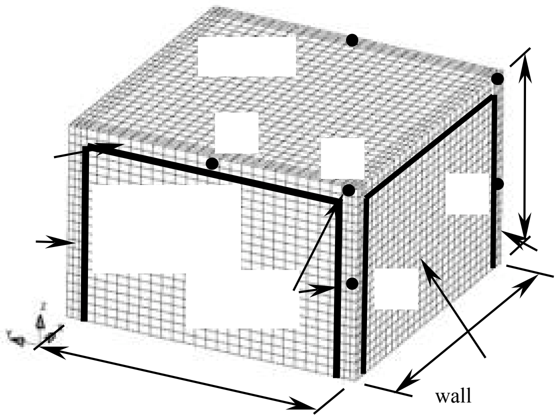

Fig. 1 Numerical model of one-storey structure and targets on the structure

Fig. 2 shows displacement distributions of the one-storey building at 0.015s after explosion at a scaled distance of 0.5 m/kg$^{1/3}$ when it is subjected to respectively the simultaneous ground shock and airblast load, and airblast load only. As shown in Fig. 2 (a), more severe damage occurs in the front and rear columns and side walls of the structural model when ground shock is included. But it is also found, not shown, that ground shock alone could not cause the structure to collapse. These results indicate that when the structure is close to the explosion centre, structural response and damage are governed by airblast load, and ground shock influence can be neglected, as most of codes and regulations do. As the scaled distance increases, airblast load decreases rapidly. At a certain scaled distance, collapse of the structure under airblast load alone will not occur. Numerical results demonstrate that the critical scaled distance is 1.84 m/kg$^{1/3}$ (see Fig. 3b). However, when the structure is under combined ground shock and airblast load at this scaled distance, failure of front columns of the structure is observed and structure collapses (see Fig. 3a), indicating that at this critical scaled distance, the ground shock influence cannot be neglected.

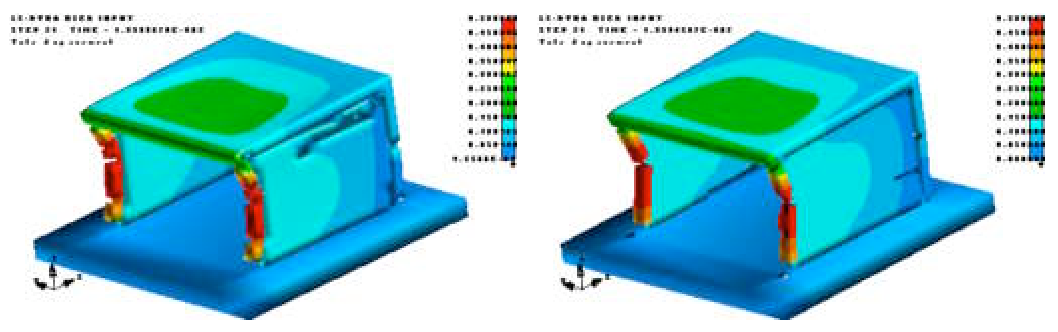

a. combined load b. airblast load

Fig. 2 Displacement distribution of the structure at 0.015s after an explosion at scaled distance 0.5 m/kg$^{1/3}$

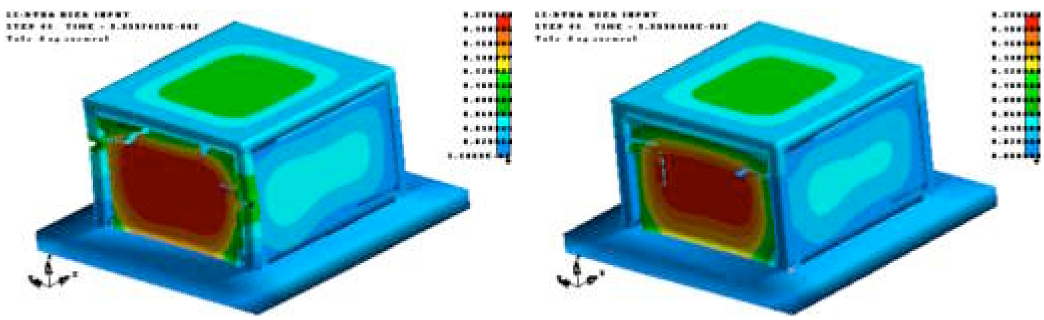

a. combined load   b. airblast load

Fig. 3 Displacement distribution of the structure at 0.05s after an explosion at scaled distance 1.84 m/kg$^{1/3}$

Fig. 4 illustrates a comparison of velocity responses of the structure at target 4 to the combined ground shock and airblast forces, ground shock only and airblast forces only when the scaled distances are 2, 3, 4 and 5 m/kg$^{1/3}$. It is clear that when the scaled distance is 2 m/kg$^{1/3}$, the peak velocity generated by ground shock is about one-tenth of that produced by airblast load. But at the scaled distance 4 m/kg$^{1/3}$, peak velocity produced by ground shock is slightly larger than that induced by airblast force. When the scaled distance increases to 5 m/kg$^{1/3}$, peak velocity induced by ground shock is larger than that produced by airblast force, and little difference is observed between velocity response of structure by airblast load and by combined load after 0.078s, implying that the structure responds to airblast load almost from rest. Therefore, when the scaled distance is more than 5 m/kg$^{1/3}$, the structural response can be analyzed separately by ground shock only as well as by airblast load only, indicating that with the increase of the scaled distance, the structural response and damage are not governed by airblast load any more. In this case, considering ground shock in the structural response and damage analysis to surface explosions is important.

5. CONCLUSION

This paper investigated the relative importance of ground shock and airblast force on structural response and damage from a surface explosion. It was found that airblast force governs the surface explosion effects on structures when structures are close to explosion centre. However, at certain critical points, neglecting ground shock effects might underestimate structural collapse potential. With the increase of the scaled distance ground shock effects increase and it eventually generates larger peak structural response than airblast force. Structure response and damage to airblast force and ground shock can be analysed separately when scaled distance is large.

6. ACKNOWLEDGEMENTS

The authors would like to acknowledge the financial support from the Australian Research Council (ARC) under grant number DP0451966 for carrying out this research work.

7. REFERENCES

British Standards Institution, BS8110. (1985) Structural use of concrete; Part 1&2, 2 Park Street, London, UK.

Dowding CH, Fulthorpe CS, and Langan RT. (1982) Simultaneous airblast and ground motion response, Journal of Structural Division, ASCE, Vol 108 (11).
Henrych, J. (1979) The Dynamics of Explosion and Its Use, Amsterdam, Oxford, New York.
Lu Y and Xu K. (2004) Modeling of dynamic behavior of concrete materials under blast loading, International Journal of Solids and Structures, Vol 41, pp131-143.
Lubliner J, Oliver J, Oller S, and Onate E. (1989) A plastic-damage model for concrete, International Journal of Solids and Structures, Vol 25 (3), pp299-326.
Technical Manual (TM-5-855-1 1986). Fundamentals of Protective Design for Conventional Weapons, Headquarters, Department of the Army, Washington DC.
Wu C and Hao H. (2004) Numerical study of relative importance of surface explosion generated airblast force and ground shock on dynamic structural response, The 18th Australasian Conference on the Mechanics of Structures and Materials, Perth, Western Australia, pp975-980.
Wu C and Hao H. (2005a) Modeling of simultaneous ground shock and airblast pressure on nearby structures from surface explosions, International Journal of Impact Engineering, Vol 31(6), pp699-717.
Wu C and Hao H. (submitted 2005b) Derivation of 3D masonry properties using numerical homogenization technique.

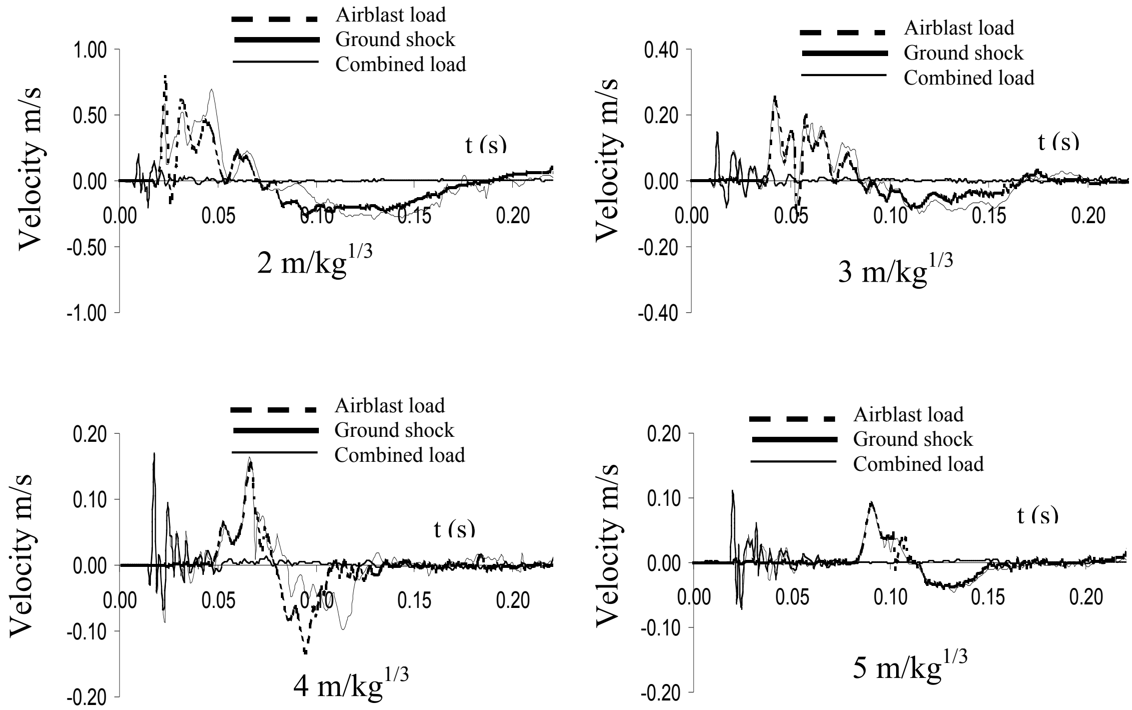

Fig. 4 Velocity response time histories at target 4 obtained by ground shock, airblast force, and combined load at different scaled distances